Supporting Information

Photosensitive Ru(II) Complexes as Inhibitors of the Major Human Drug Metabolizing Enzyme CYP3A4

Nicholas Toupin,[1] Sean J. Steinke,[2] Sandeep Nadella,[1] Ao Li,[1] Thomas N. Rohrabaugh, Jr., [2] Eric R. Samuels,[3#] Claudia Turro, [2,*] Irina F. Sevrioukova,[4,*] and Jeremy J. Kodanko[1,5,*]

[1]Department of Chemistry, Wayne State University, 5101 Cass Ave, Detroit, MI 48202,

[2]Department of Chemistry and Biochemistry, The Ohio State University, Columbus, Ohio 43210,

[3]Departments of Pharmaceutical Sciences and [4]Molecular Biology and Biochemistry, University of California, Irvine, CA 92697

[5]Barbara Ann Karmanos Cancer Institute, Detroit, Michigan 48201

Table of Contents

1. Compound Synthesis and Characterization

Scheme S1. Synthesis of 4

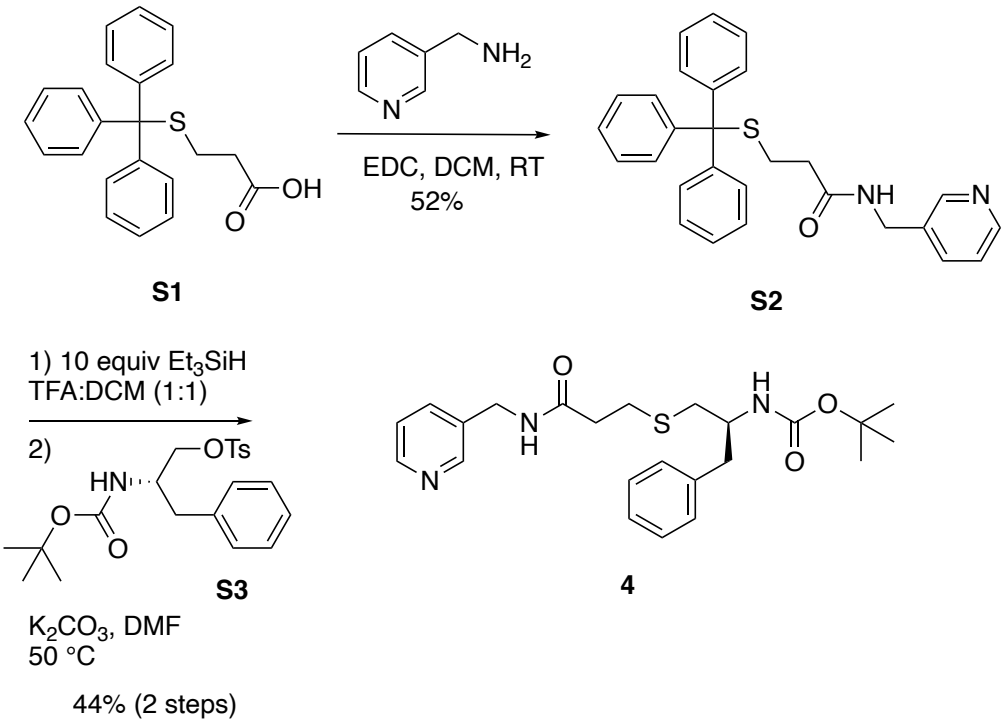

***N*-(pyridin-3-ylmethyl)-3-(tritylthio)propanamide (S2).** To a solution of EDC (110 mg, 0.58 mmol) in DCM (16 mL), 3-(tritylthio)propionic acid (**S1**, 200 mg, 0.580 mmol) was added. While stirring, 3-picolylamine (0.060 mL, 0.580 mmol) was added to the mixture. The resulting reaction mixture was stirred at room temperature for 16 h under nitrogen atmosphere. Upon completion, the mixture was washed with saturated $NaHCO_3$ solution. The organic layer was dried over Na_2SO_4 and concentrated under reduced pressure. The crude product was then purified over silica (5% MeOH/EtOAc) to give S**2** as a colorless oil (170 mg, 68%): ^{1}H NMR (400 MHz $CDCl_3$) δ 8.52 (s, 1H), 8.48 (d, 1H, J = 4.4 Hz), 7.69 (d, 1H, J = 8.0 Hz), 7.39 (d, 6H, J = 7.6 Hz), 7.30–7.24 (m, 6H), 7.23–7.18 (m, 4H), 6.07 (s, 1H), 4.38 (d, 2H, J = 6.0 Hz), 2.52 (t, 2H, J = 7.2 Hz), 2.09

(t, 2H, J = 7.2 Hz); ^{13}C NMR (100 MHz $CDCl_3$) δ 171.2, 148.1, 147.7, 144.6, 136.8, 134.6, 129.5, 128.0, 126.7, 123.9, 66.9, 40.9, 35.5, 27.6; ESMS calcd for $C_{28}H_{27}N_2OS$ ($[M+H]^+$) 439; found 439.

***tert*-butyl (*S*)-(1-((3-oxo-3-((pyridin-3-ylmethyl)amino)propyl)thio)-3-phenylpropan-2-yl)carbamate (4).** To a solution of compound **S2** (133 mg, 0.300 mmol) in DCM (9.0 mL), TFA (9.0 mL) was added. While stirring, triethylsilane (0.490 mL, 3.03 mmol) was added slowly to the obtained yellow-colored solution. The mixture was stirred at room temperature for 1 h under a nitrogen atmosphere until the yellow color disappeared. The reaction mixture was concentrated under reduced pressure. The thiol intermediate was obtained after recrystallization (EtOAc/cold hexanes). Without further purification, the thiol intermediate (110 mg, 0.560 mmol) was added to a solution of K_2CO_3 (155 mg, 1.12 mmol) and **S3**[1] (152 mg, 0.380 mmol) in DMF. The reaction mixture was heated at 50 °C for 3 h. Upon completion, the reaction mixture was extracted with EtOAc and washed with ice-cold water. The organic layer was collected, dried over Na_2SO_4 and concentrated under reduced pressure. The crude product was purified over silica (10% MeOH/EtOAc) to give the title compound as colorless oil (57 mg, 44%): ^{1}H, ^{13}C NMR and ESMS data agreed with data for **4** from the literature.[1]

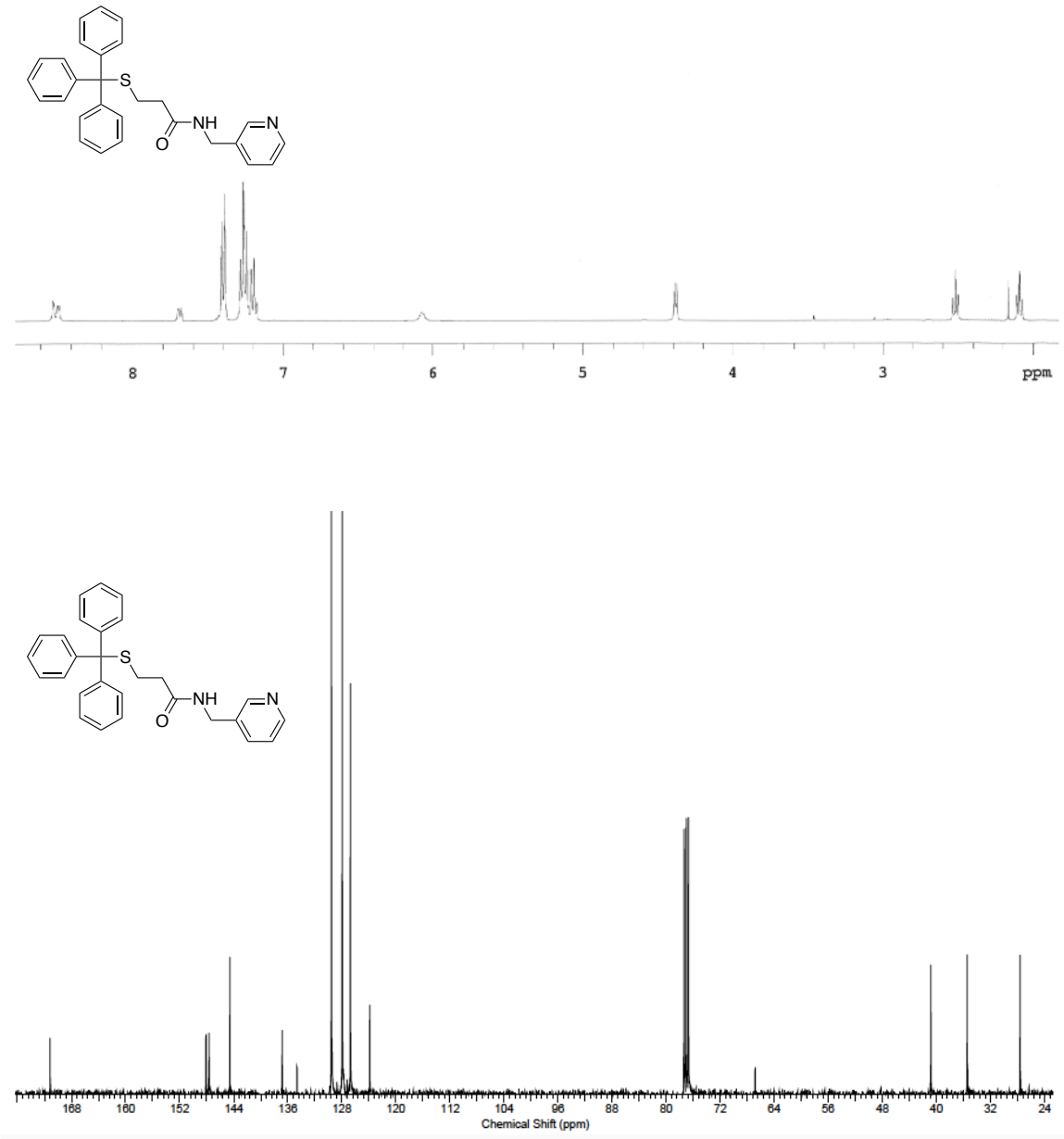

Figure S1. ^{1}H NMR spectrum (top) of compound **2** in $CDCl_3$ and ^{13}C NMR spectrum (bottom) of compound **2** in $CDCl_3$.

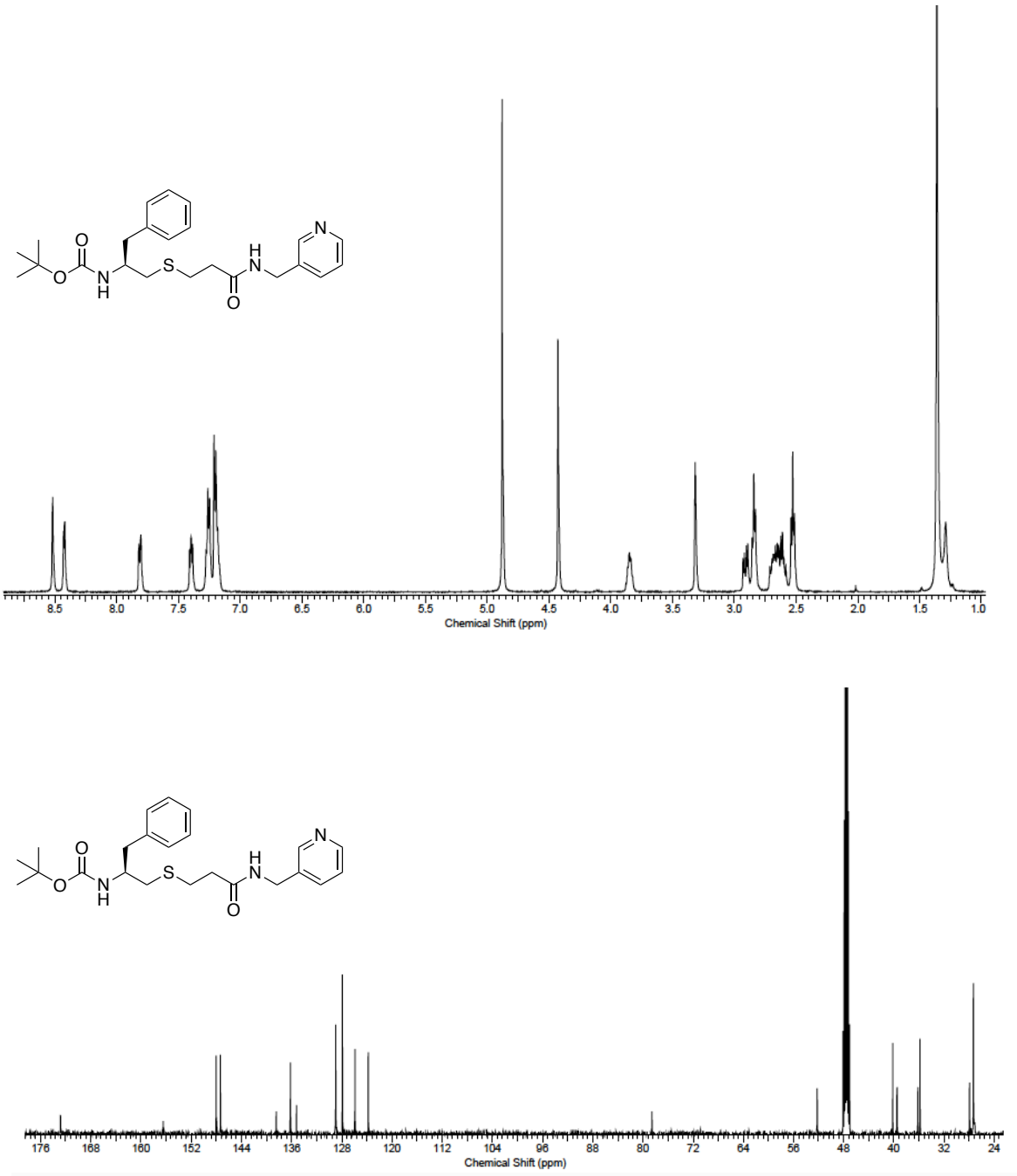

Figure S2. ^{1}H NMR spectrum (top) of compound **4** in CD_3OD and ^{13}C NMR spectrum (bottom) of compound **4** in CD_3OD.

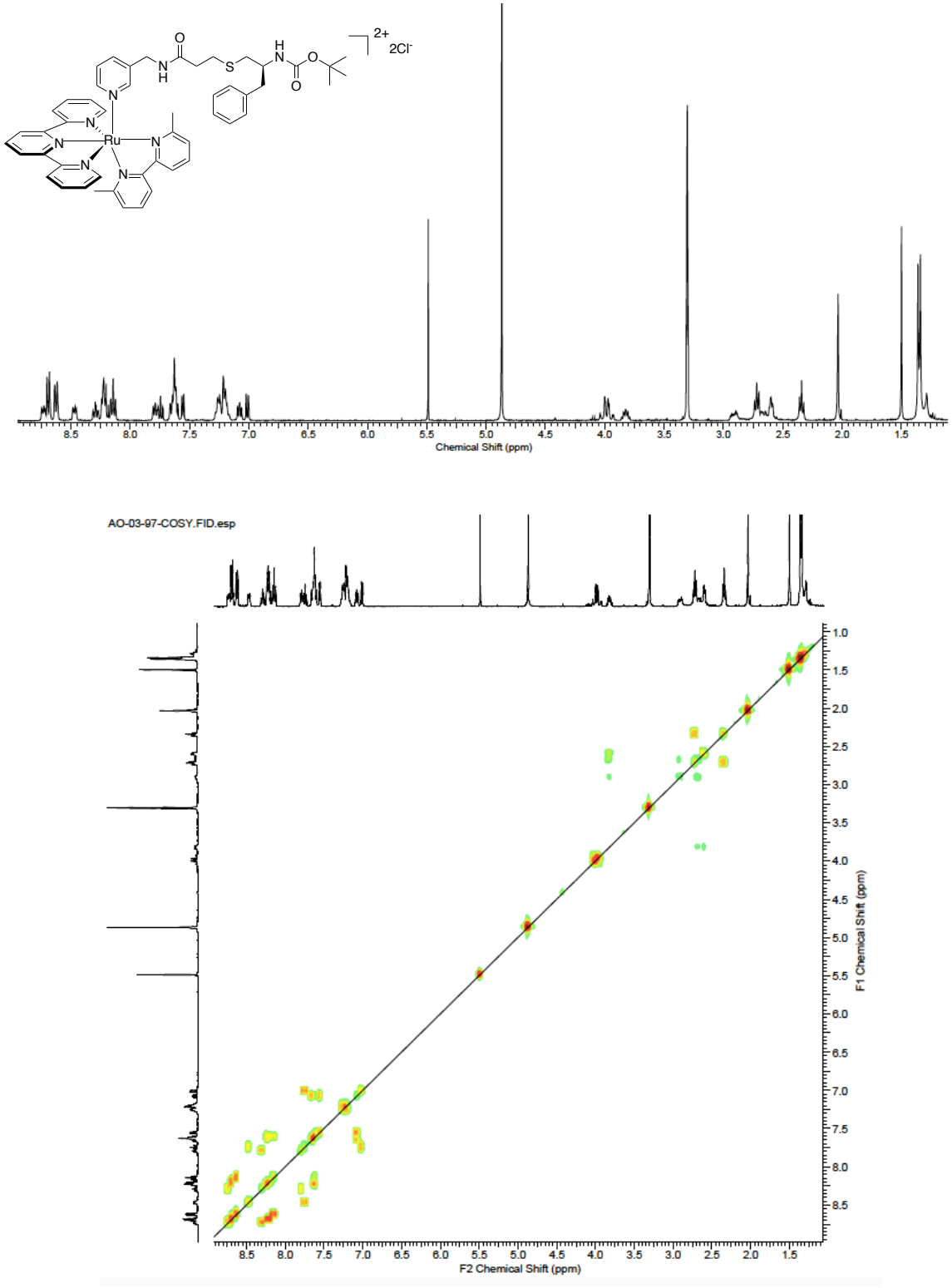

Figure S3. ^{1}H NMR spectrum (top) of complex **7** in CD_3OD and COSY spectrum (bottom) of complex **7** in CD_3OD.

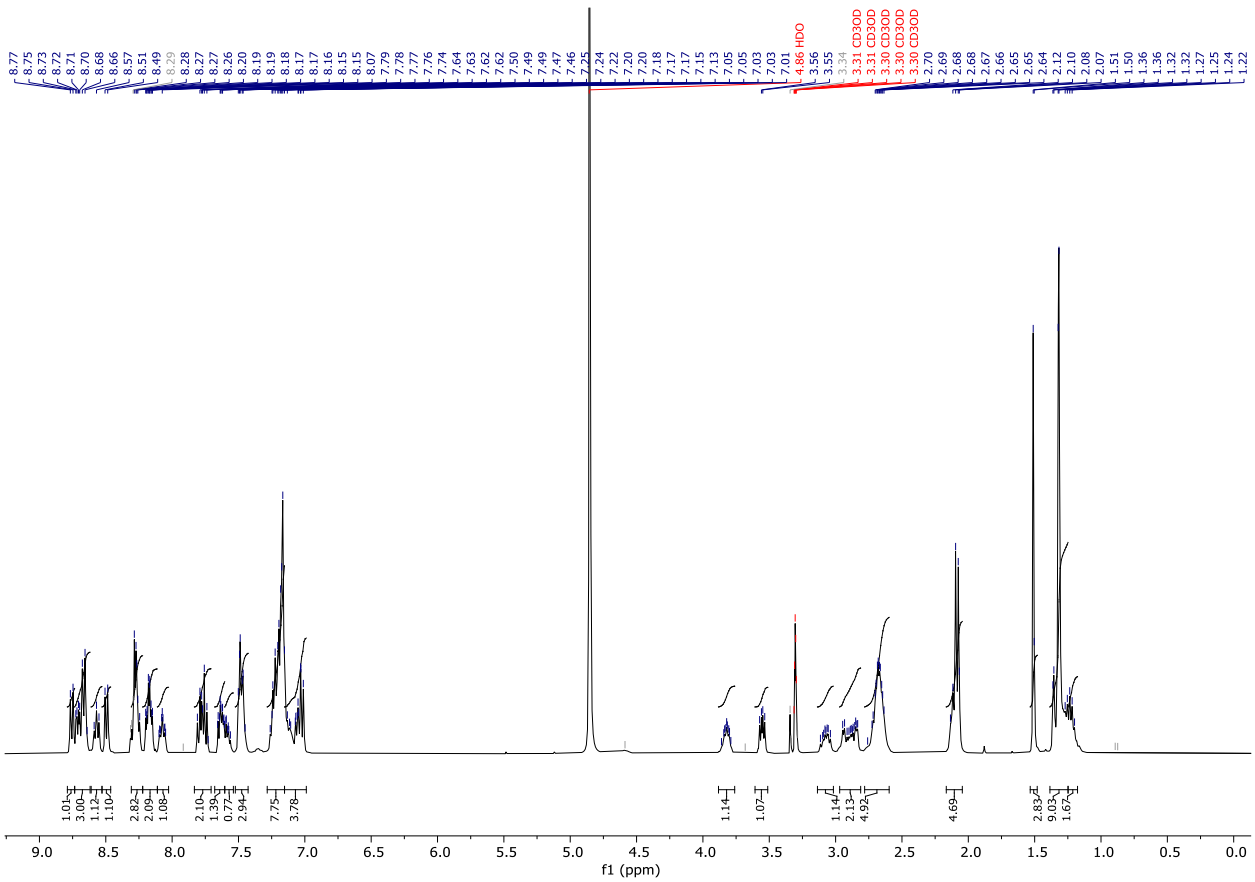

Figure S4. ^{1}H NMR spectrum of **8** in CD_3OD

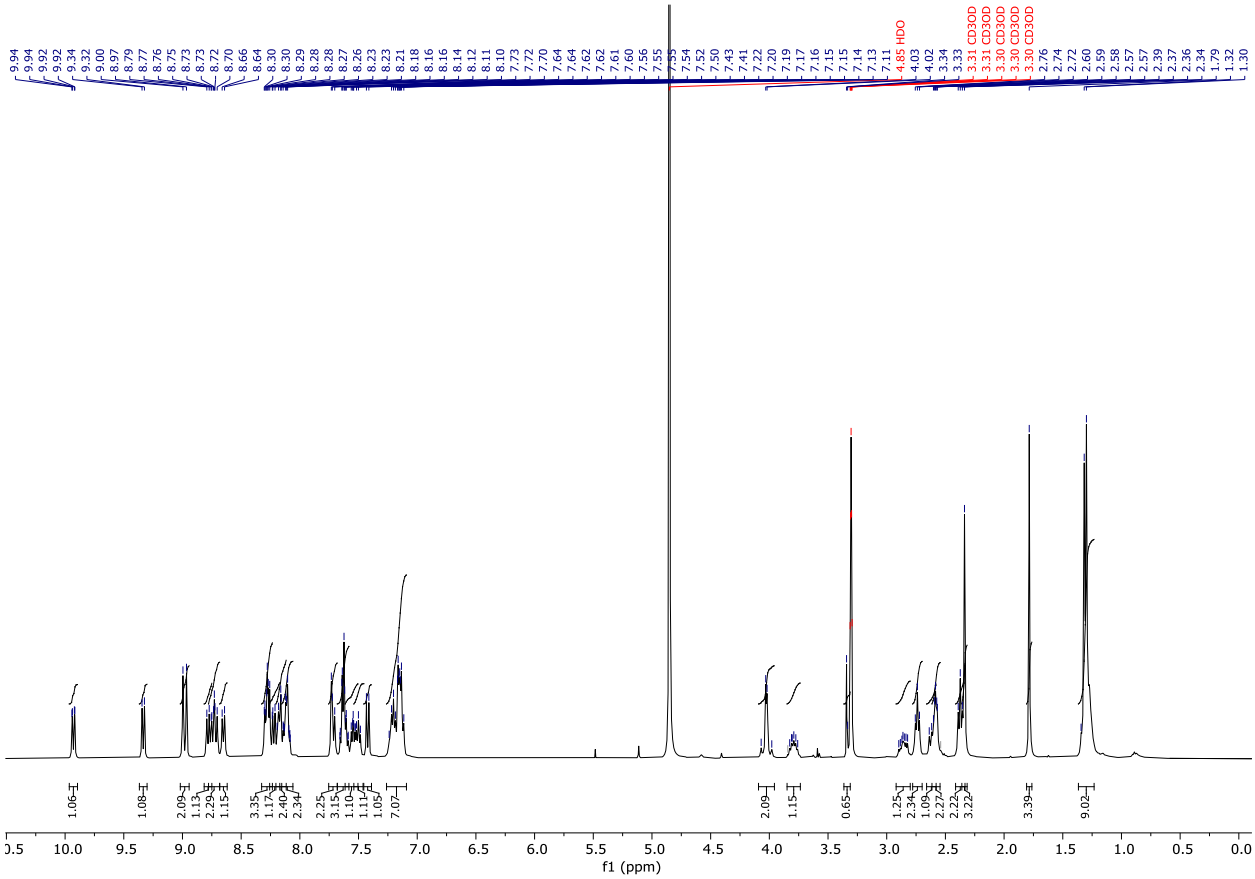

Figure S5. ^{1}H NMR spectrum of **9** in CD_3OD

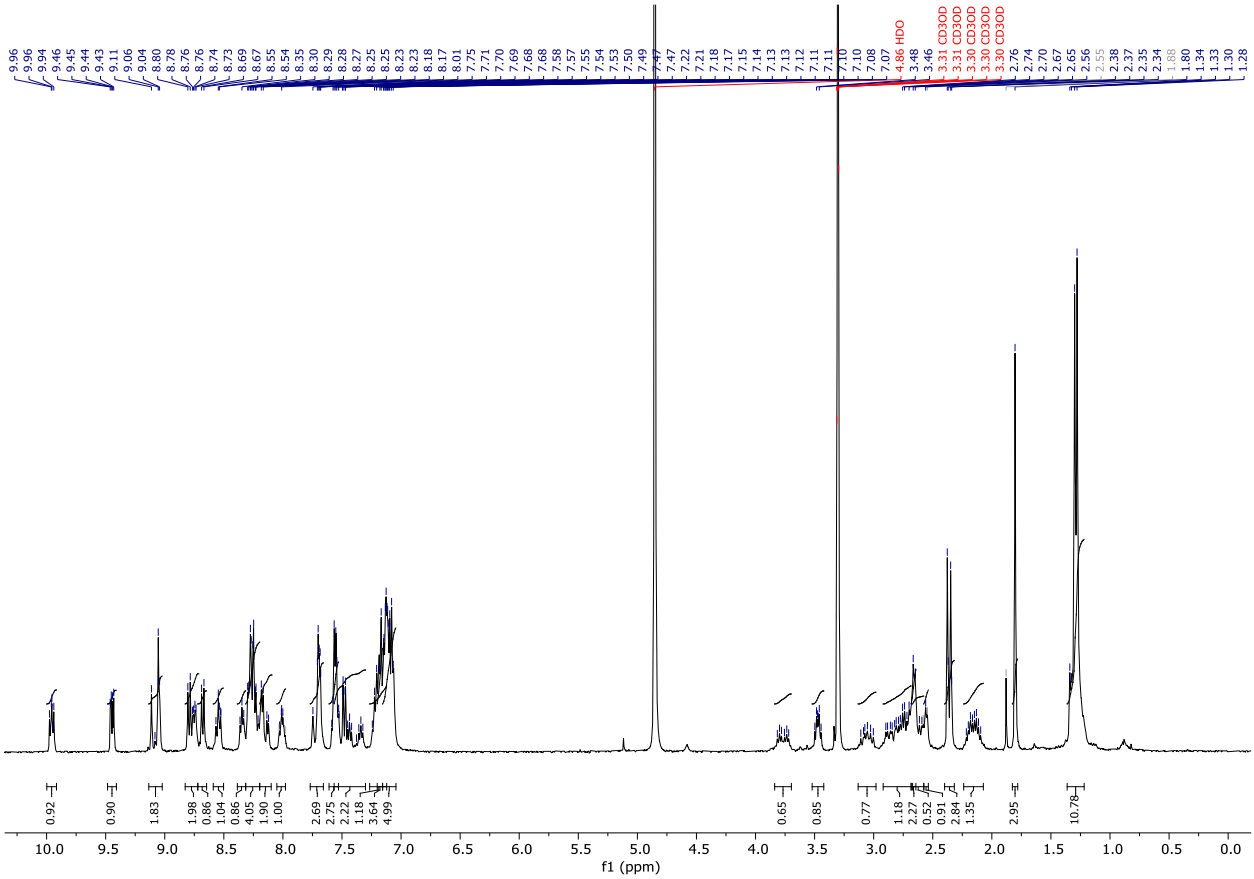

Figure S6. ^{1}H NMR spectrum of **10** in CD_3OD

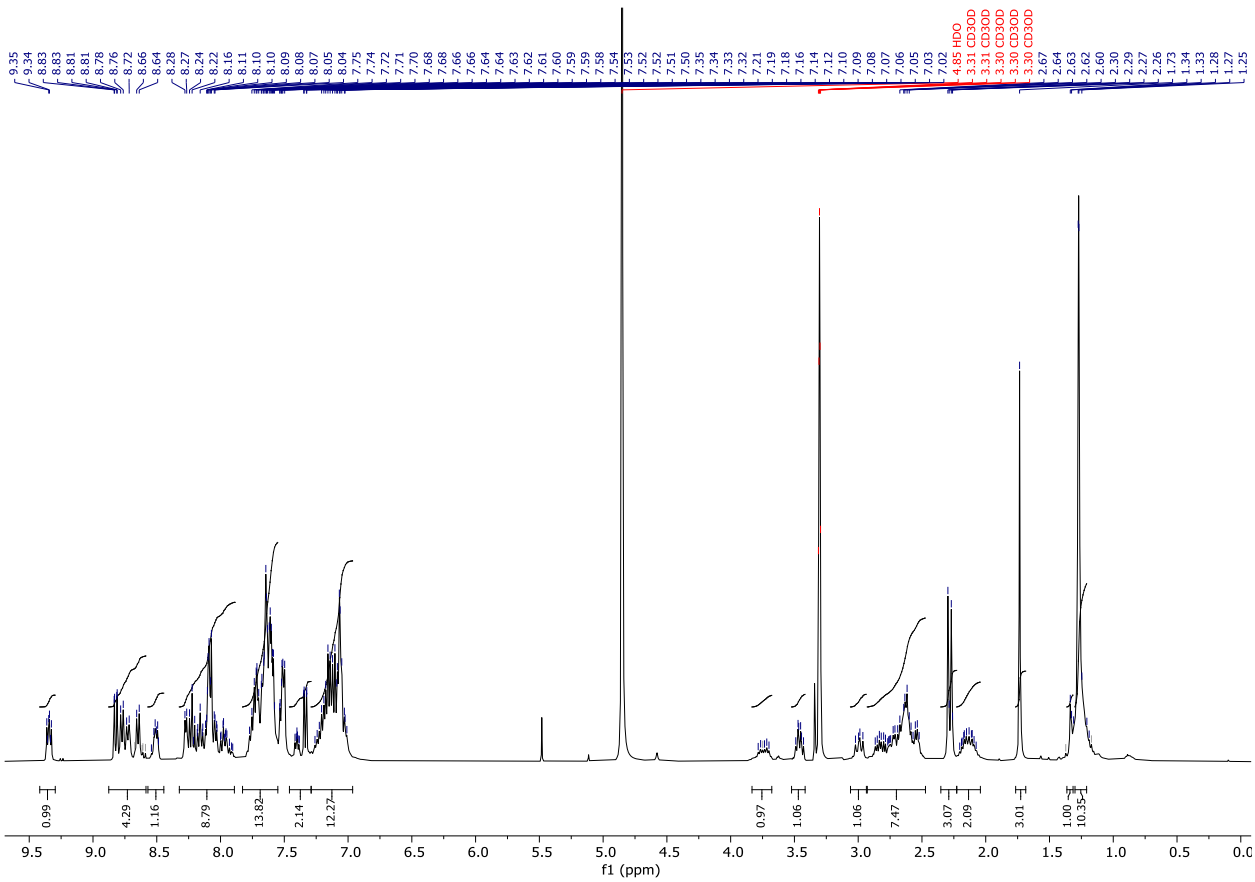

Figure S7. ^{1}H NMR spectrum of **11** in CD_3OD

2. Photochemical Studies

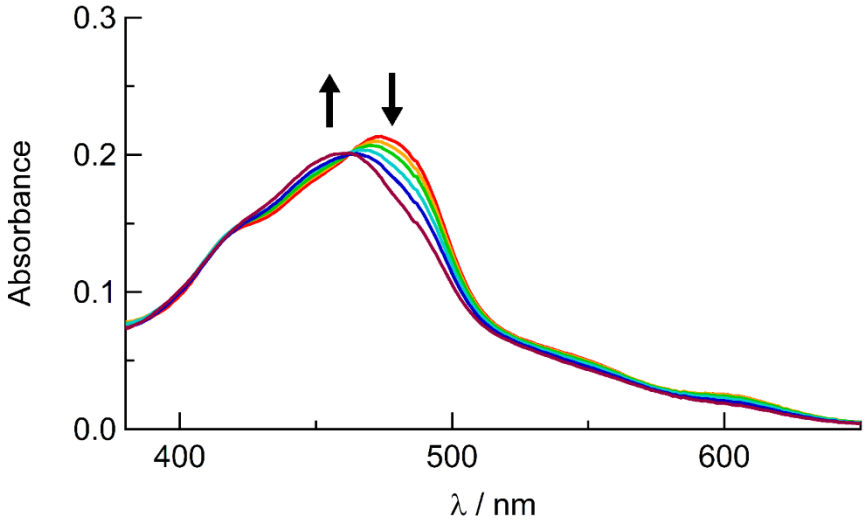

Figure S8. Changes in the electronic absorption spectrum of **8** in CH_3CN following irradiation (λ_{irr} = 500 nm) under an Ar atmosphere, t_{irr} = 0 – 10 min.

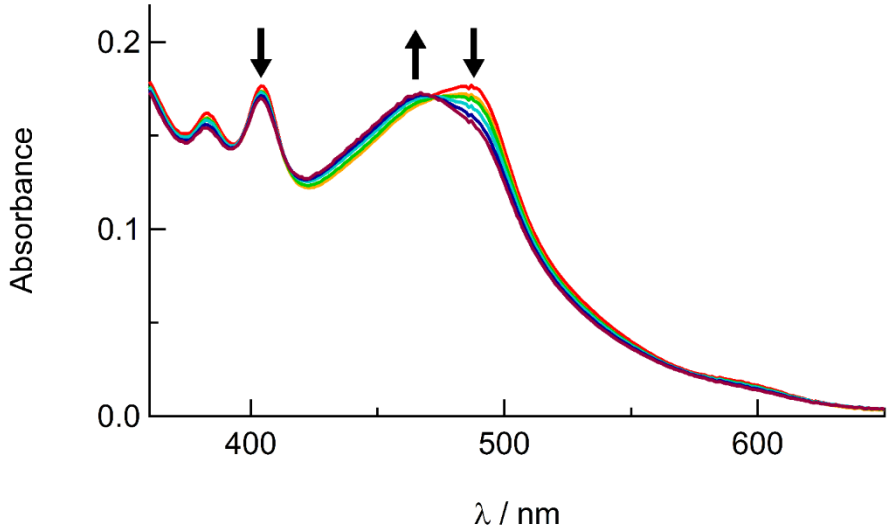

Figure S9. Changes in the electronic absorption spectra of **9** in CH_3CN following irradiation (λ_{irr} = 500 nm) under an Ar atmosphere, t_{irr} = 0 – 8 min

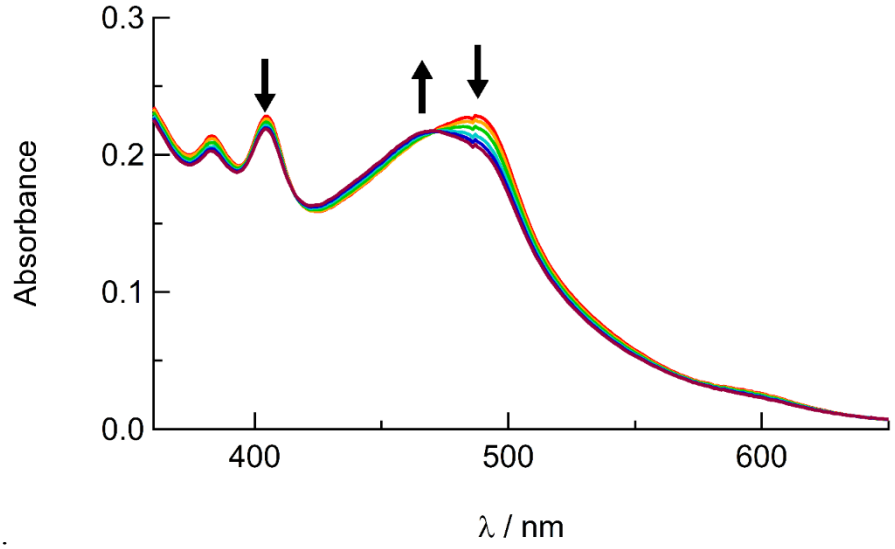

Figure S10. Changes in the electronic absorption spectra of **10** in CH_3CN following irradiation (λ_{irr} = 500 nm) under an Ar atmosphere, t_{irr} = 0 – 10 min.

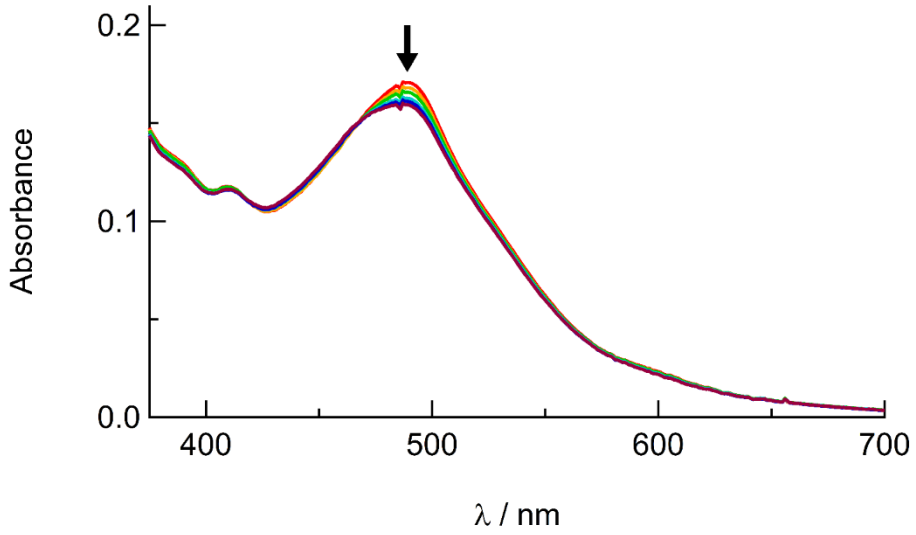

Figure S11. Changes in the electronic absorption spectra of **11** in CH_3CN following irradiation (λ_{irr} = 500 nm) under an Ar atmosphere, t_{irr} = 0 – 8 min.

3. Structural Studies

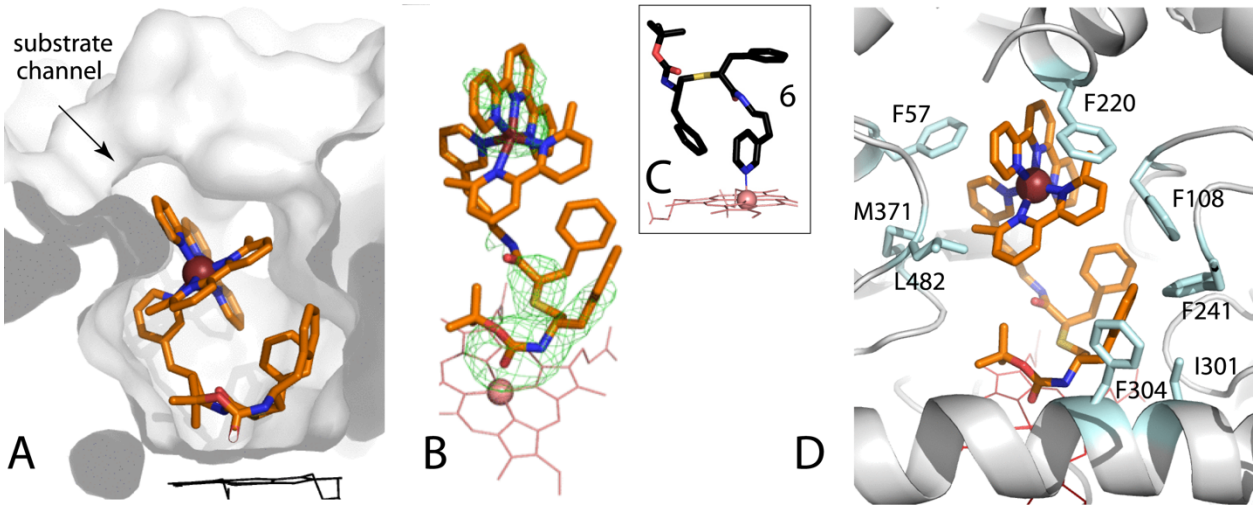

Figure S12. Crystal structure of CYP3A4 bound to the intact caged compound **8** at 2.5 Å resolution. **A**, Orientation of 8 in the active site. **B**, Omit electron density rendered around **8** at 3σ level (shown in green mesh). **C**, Orientation of free **6** in the active site of CYP3A4 (7KVH structure) shown for comparison. **D**, Aromatic and hydrophobic residues stabilizing the CYP3A4-**8** inhibitory complex.

Table S1. X-day data collection and model refinement statistics

Ligand	**7**	**8**
PDB ID	7KS8	7KSA
Data statistics		
Space group	I222	I222
Unit cell parameters	*a* = 77 Å, *b* = 101 Å, *c* = 127 Å; α, β, γ = 90°	*a* = 75 Å, *b* = 95 Å, *c* = 121 Å; α, β, γ = 90°
Molecules per asymmetric unit	1	1
Resolution range (Å)	79.23 - 2.50 (2.64 – 2.50)[a]	74.88 - 2.50 (2.64 – 2.50)
Total reflections	66,754	73,951
Unique reflections	16,978	15,117
Redundancy	3.9 (3.9)	4.9 (4.9)
Completeness	97.3 (98.0)	99.0 (99.6)
Average $I/\sigma I$	7.3 (0.9)	10.4 (1.1)
R_{merge}	0.070 (2.562)	0.061 (1.672)
R_{pim}	0.038 (1.234)	0.030 (0.825)
CC ½	0.996 (0.306)	0.999 (0.302)
Refinement statistics		
R/R_{free}[b]	21.1/26.2	22.8/26.6
Number of atoms:		
Protein	3641	3548
Solvent	0	9
R.m.s. deviations:		
Bond lengths, Å	0.011	0.009
Bond angles, °	1.155	0.956
Wilson B-factor, Å^2	85	83
Average *B*-factor, Å^2:		
Protein	107	125
Ligand	109	187
Ramachandran plot[c] (residues; %)		
Preferred	428 (96.0%)	402 (92.6%)
Allowed	17 (4.0%)	31 (7.2%)
Outliers	0	1 (0.2%)

[a] Values in brackets are for the highest resolution shell.
[b] R_{free} was calculated from a subset of 5% of the data that were excluded during refinement.
[c] Analyzed with PROCHECK.

4. Biological Studies

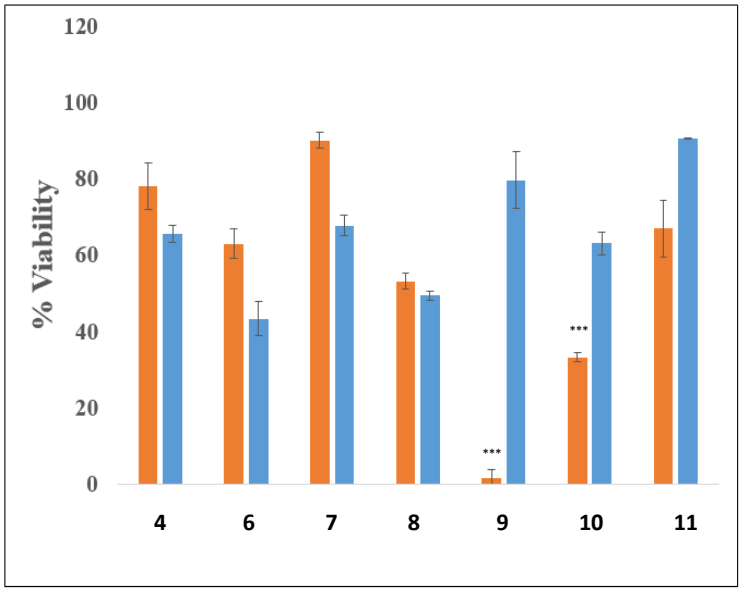

Figure S13: DU-145 cells were seeded in a 96-well plate at a density of 7000 cells per well and incubated overnight (~18 h). The media was aspirated from each well and quadruplicate wells were treated with media containing one of compounds **4** or **6-11** (5 μM) in 1% DMSO with vinblastine co-treatment (5 nM). After 1 h incubation at 37 °C, the plates were irradiated using a blue LED light source (t_{irr} = 20 min, λ_{irr} = 460–470 nm) (**Orange**) or left in the dark (**Blue**) and incubated for 72 h. MTT assay was then performed. Viability data were obtained by averaging blank-normalized absorbance values for control cells and expressing average absorbance for the treated samples as percent control. P-values are vs. dark viabilities for each compound; $^{***}P< 0.01$ $^{**}P< 0.05$ $^{*}P< 0.10$.

		Compound 27			
		10 µM	**5 µM**	**2.5 µM**	**1 µM**
Vinblastine	**10 nM**	0.4793	0.4601	0.6999	0.8307
	5 nM	0.5423	0.6211	1.1318	2.0838
	2.5 nM	0.769	2.08	>10	5.4274
	1 nM	0.6343	0.8954	>10	>10
	0.5 nM	0.771	1.2049	1.2833	>10

Figure S14: Chou-Talalay determination of drug synergy between **27** and vinblastine. Values shown in colored boxes denote combination indices (CI). CI > 1: antagonism, CI = 1: additive effect, CI < 1: synergy. CI Values were obtained using Compusyn software.

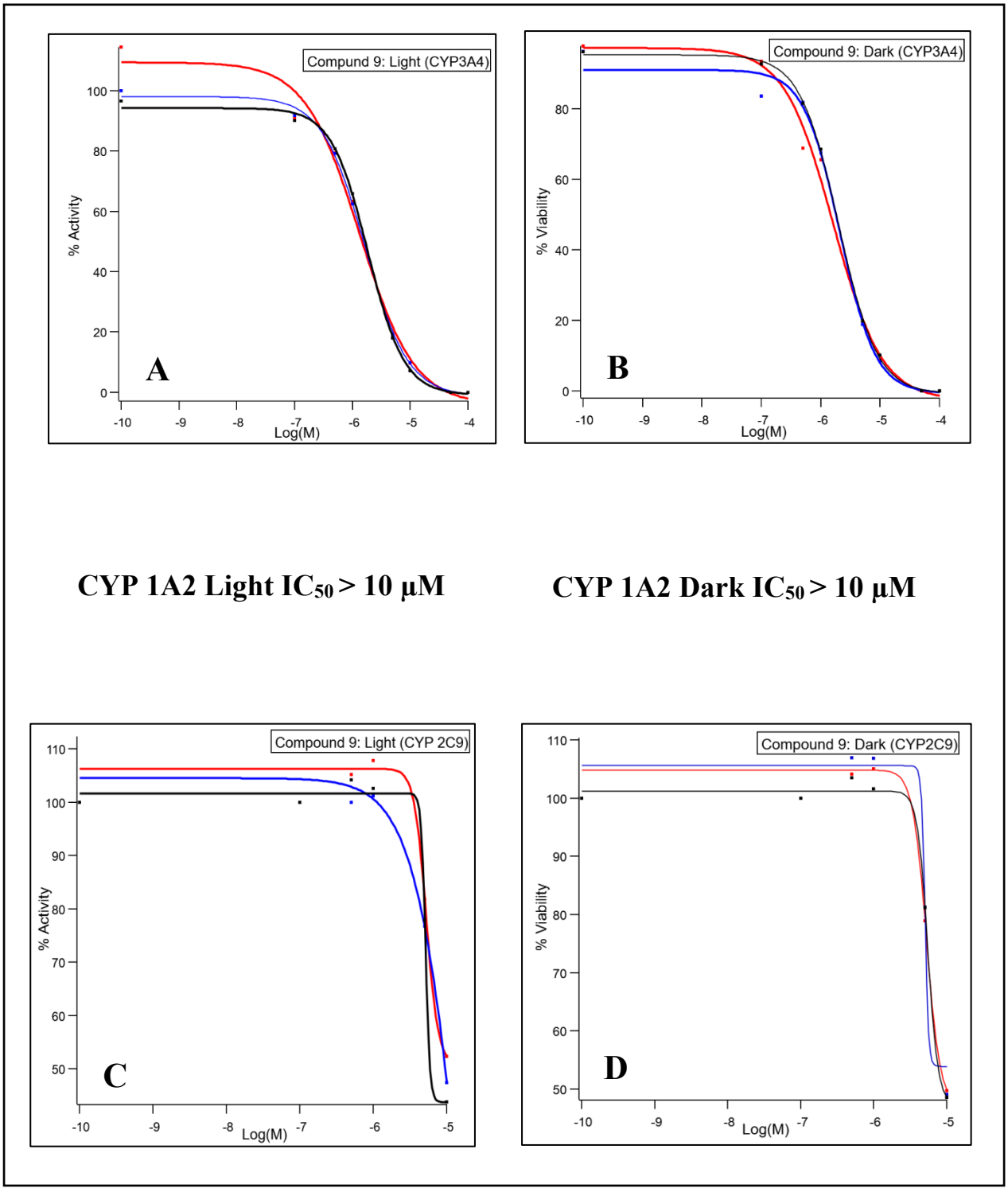

Figure S15: IC_{50} Plots were constructed using data obtained from CYP3A4, (**A**: Light, **B**: Dark) CYP1A2 (**ND**) or CYP2C9 (**C**: Light, **D**: Dark) Inhibitor Screening Kits (BioVision) following manufacturer protocols. Stock solutions of **9** were prepared in MeCN, plated and combined with assay buffer and irradiated with a blue LED light source (t_{irr} = 20 min, λ_{irr} = 460–470 nm) or left in the dark. Experiments with compound **9** did not exceed 10 µM due to solubility limitations in assay buffer.

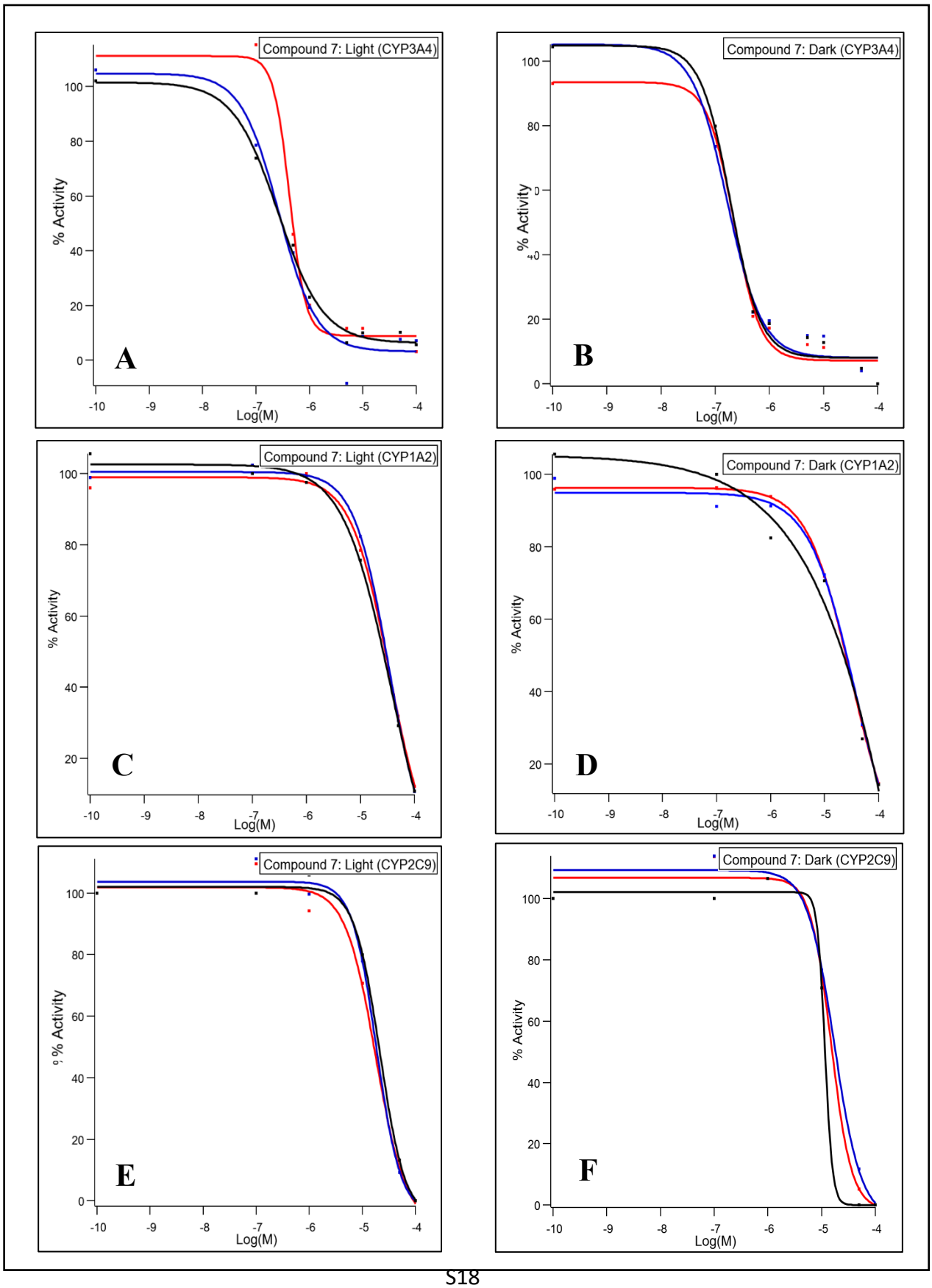
Compound 7: Light (CYP3A4)
% Activity
Log(M)
A
Compound 7: Dark (CYP3A4)
% Activity
Log(M)
B
Compound 7: Light (CYP1A2)
% Activity
Log(M)
C
Compound 7: Dark (CYP1A2)
% Activity
Log(M)
D
Compound 7: Light (CYP2C9)
% Activity
Log(M)
E
Compound 7: Dark (CYP2C9)
% Activity
Log(M)
F

Figure S16: IC_{50} Plots were constructed using data obtained from CYP3A4, (**A**: Light, **B**: Dark) CYP1A2 (**C:** Light, **D**: Dark) or CYP2C9 (**E**: Light, **F**: Dark) Inhibitor Screening Kits (BioVision) following manufacturer protocols. Stock solutions of **7** were prepared in MeCN, plated and combined with assay buffer and irradiated with a blue LED light source (t_{irr} = 20 min, λ_{irr} = 460–470 nm) or left in the dark.

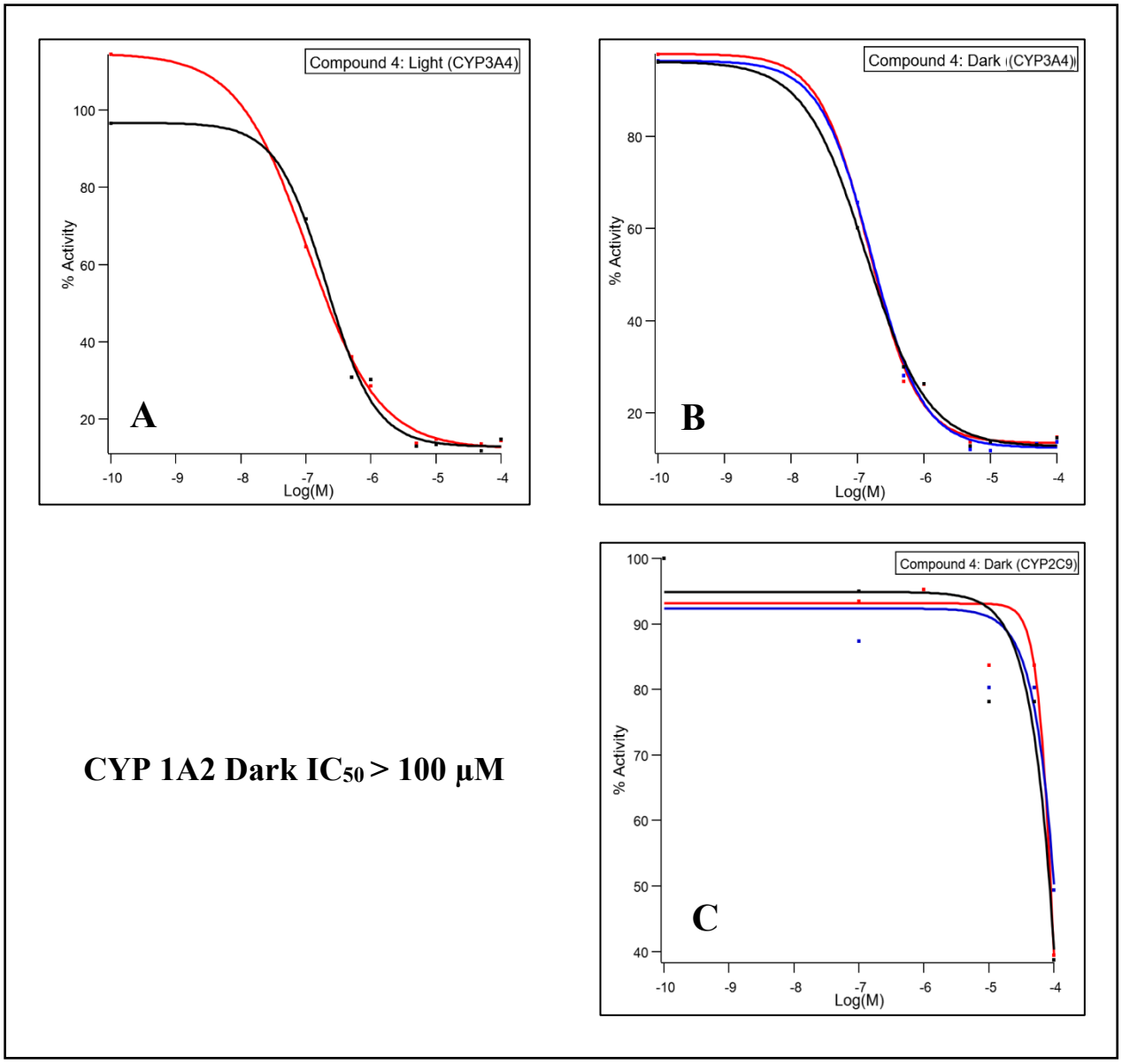

Figure S17: IC_{50} Plots were constructed using data obtained from CYP3A4, (**A**: Light, **B**: Dark) CYP1A2 or CYP2C9 (**C**: Dark) Inhibitor Screening Kits (BioVision) following manufacturer protocols. Stock solutions of **4** were prepared in MeCN, plated and combined with assay buffer and irradiated with a blue LED light source (t_{irr} = 20 min, λ_{irr} = 460–470 nm) or left in the dark

5. Stability Studies

Stock solutions of compounds **7-12** (10 μM) were prepared in phenol red free Dulbecco's modified Eagle's medium (DMEM) at room temperature. UV-vis absorbance spectra were collected after solution preparation. Vials containing stock solution were wrapped in foil to prevent interaction with light and incubated at 37 ºC for 23.5 h. Vials were then removed from the incubator and equilibrated to room temperature for 30 min followed by absorbance spectra measurements. Vials were then incubated for another 23.5 h in the 37 °C incubator and equilibrated at room temperature for 30 min, followed by measurement of the final absorbance spectra.

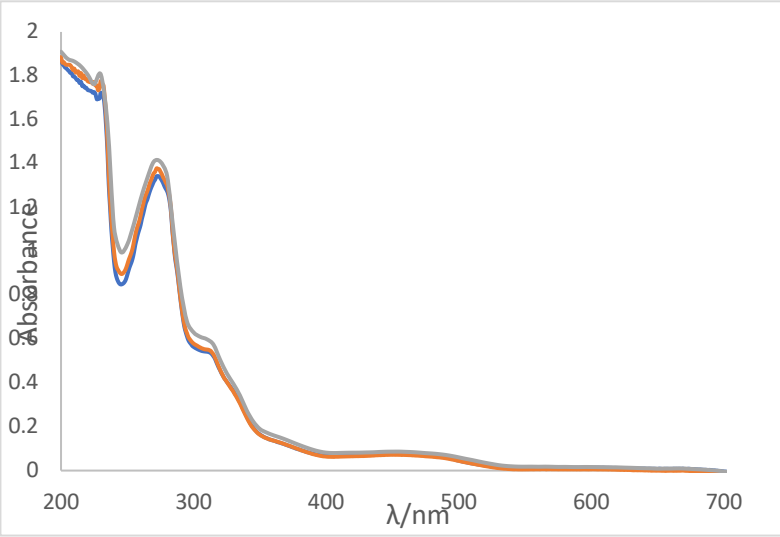

Figure S18: UV/vis absorbance spectra of **7** recorded in DMEM media before (**Blue**) and after incubation at 37 ºC for 24 h (**Orange**) and 48 h (**Gray**).

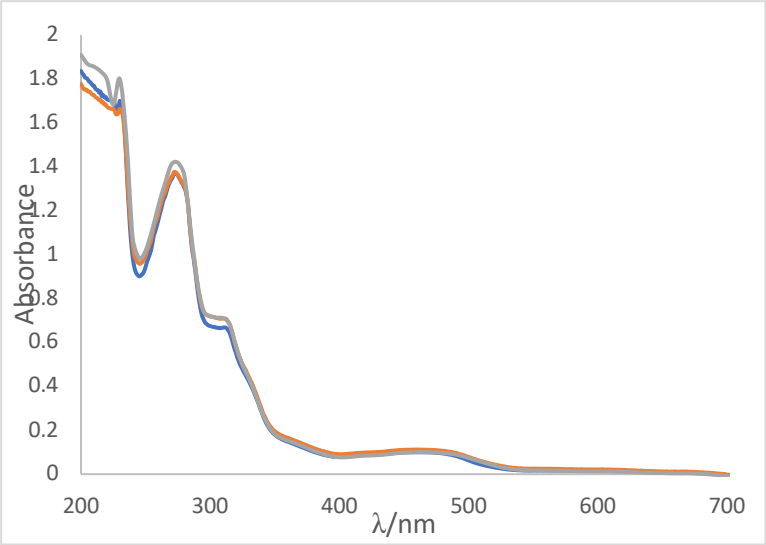

Figure S19: UV/vis absorbance of **8** in DMEM media before (**Blue**) and after incubation at 37 ^{o}C for 24 h (**Orange**) and 48 h (**Gray**).

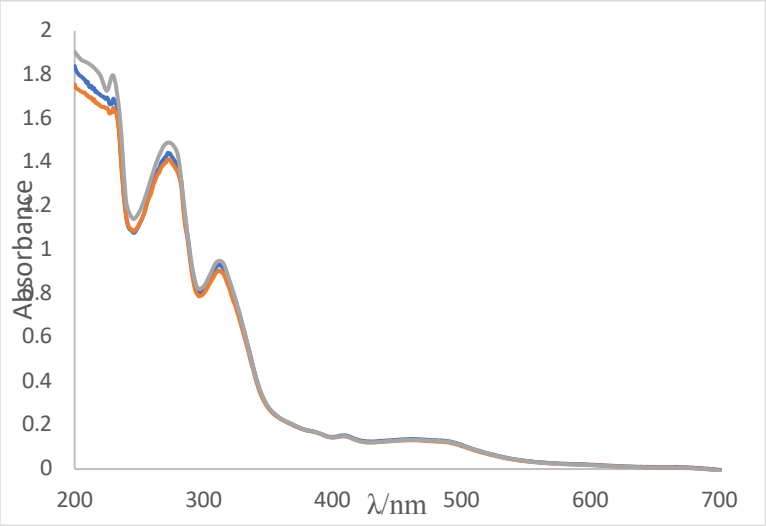

Figure S20: UV/vis absorbance of **9** in DMEM media before (**Blue**) and after incubation at 37 ^{o}C for 24 h (**Orange**) and 48 h (**Gray**) .

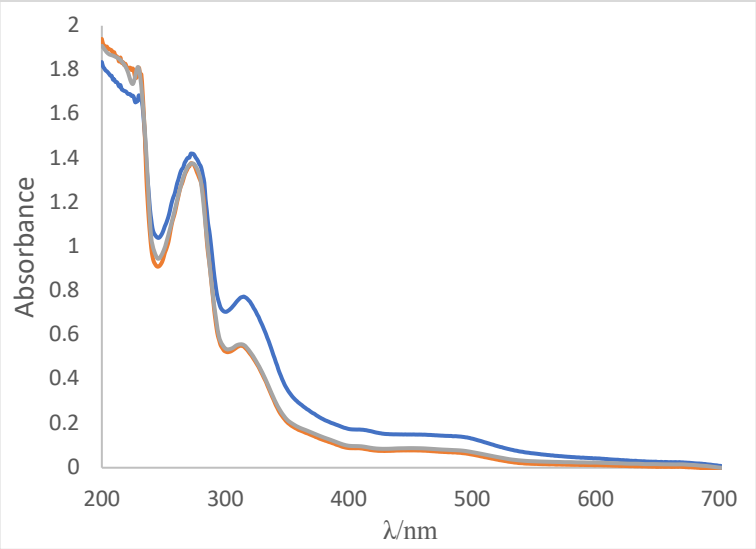

Figure S21: UV/vis absorbance of **10** in DMEM media before (**Blue**) and after incubation at 37 ^{o}C for 24 h (**Orange**) and 48 h (**Gray**) .

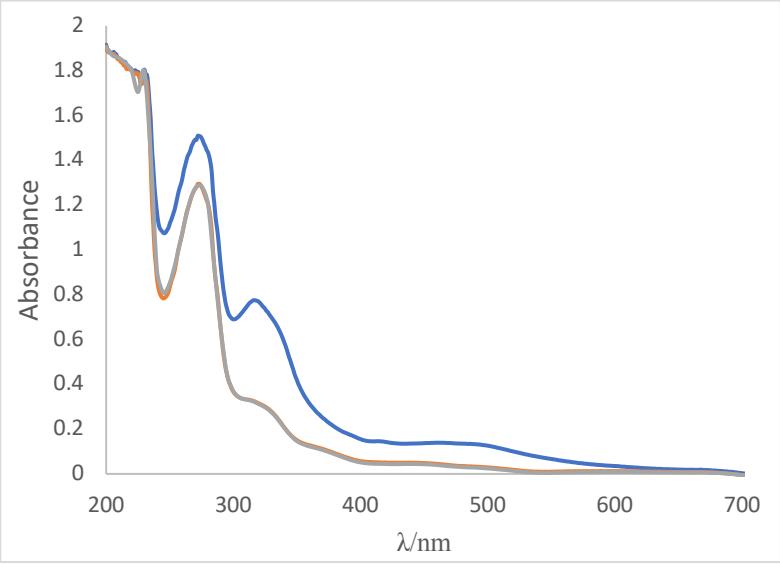

Figure S22: UV/vis absorbance of **11** in DMEM media 0 h (**Blue**), 24 h (**Orange**), and 48 h (**Gray**) post incubation at 37 ^{o}C.

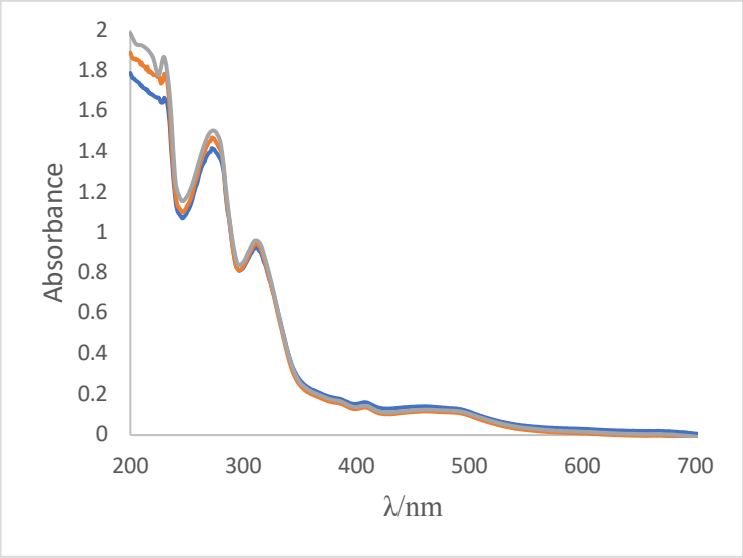

Figure S23: UV/vis absorbance of **12** in DMEM media 0 h (**Blue**), 24 h (**Orange**), and 48 h (**Gray**) post incubation at 37 ºC.

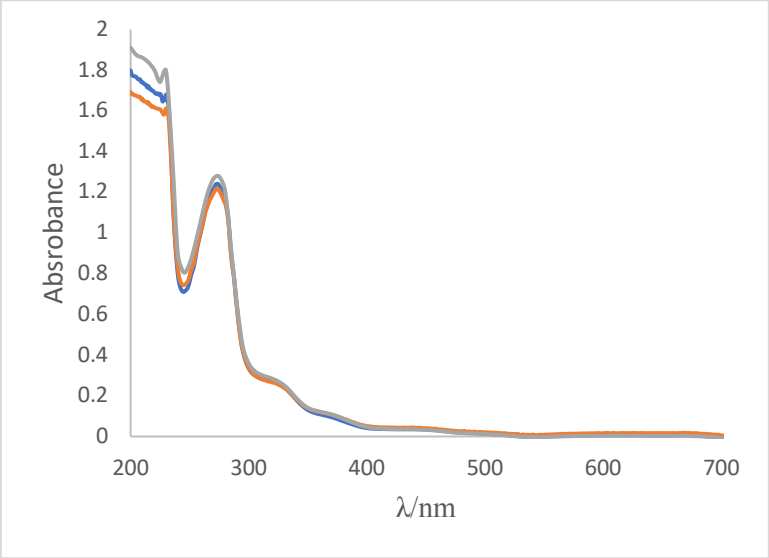

Figure S24: UV/vis absorbance of DMEM media 0 h (**Blue**), 24 h (**Orange**), and 48 h (**Gray**) post incubation at 37 ºC.

6. Compound Structures

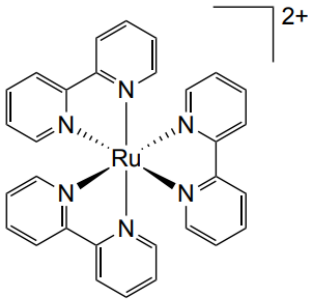

$[Ru(bpy)_3]Cl_2$ (**12**)

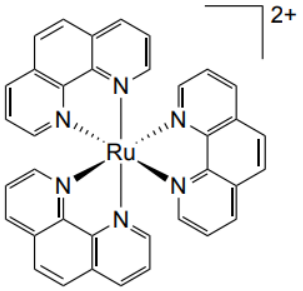

$[Ru(phen)_3](PF_6)_2$ (**13**)

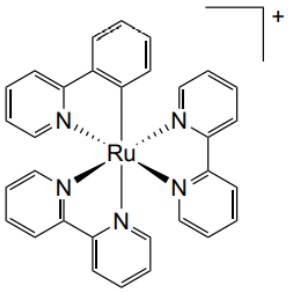

$[Ru(bpy)_2(phpy)]Cl$ (**14**)

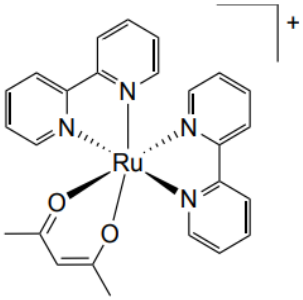

$[Ru(bpy)_2(acac)]PF_6$ (**15**)

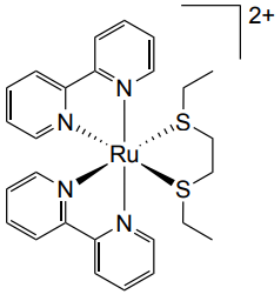

$[Ru(bpy)_2(bete)](PF_6)_2$ (**16**)

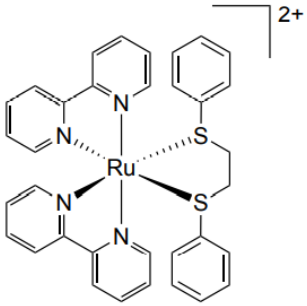

$[Ru(bpy)_2(bpte)]Cl_2$ (**17**)

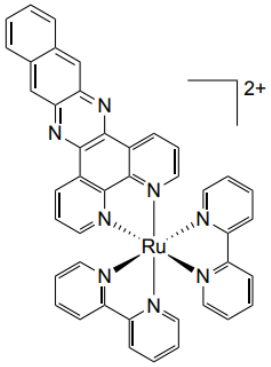

$[Ru(bpy)_2(dppn)](PF_6)_2$ (**18**)

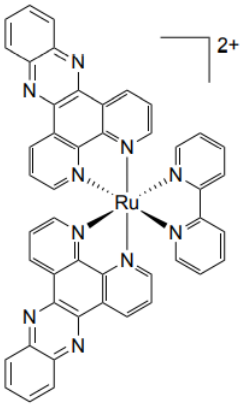

$[Ru(dppz)_2(bpy)]Cl_2$ (**19**)

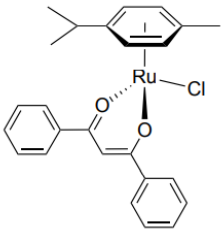

[Ru(η^6-p-cym)(DBM)Cl] (**20**)

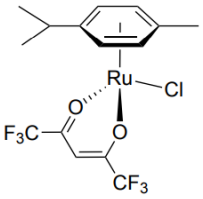

[Ru(η^6-p-cym)(hfa)Cl] (**21**)

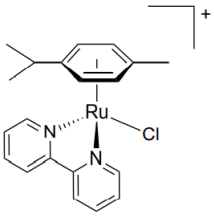

[Ru(η^6-p-cym)(bpy)Cl]Cl (**22**)

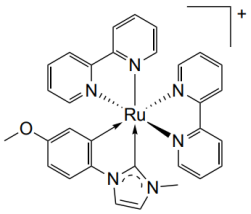

[Ru(bpy)$_2$(NHC-OMe)]PF$_6$ (**23**)

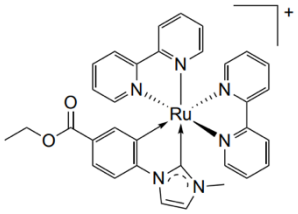

[Ru(bpy)$_2$(NHC-COOEt)]PF$_6$ (**24**)

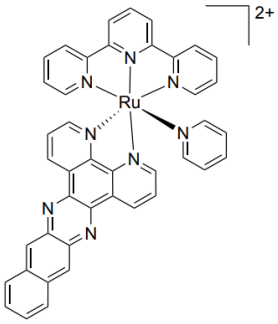

[Ru(tpy)(dppn)(py)](PF$_6$)$_2$ (**25**)

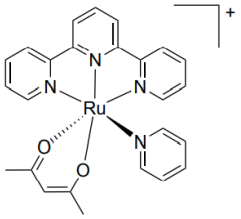

[Ru(tpy)(acac)(py)]PF$_6$ (**26**)

Figure S25: Structures of ruthenium complexes **12-26**

References.

1. Kaur, P.; Chamberlin, A. R.; Poulos, T. L.; Sevrioukova, I. F., Structure-Based Inhibitor Design for Evaluation of a CYP3A4 Pharmacophore Model. *J. Med. Chem.* **2016,** *59* (9), 4210-4220.